



# Synthesis and Study of 4-Phenylsulfonyl-2,3,5,6-tetrachloropyridine Structure

<sup>1</sup>Rakesh Vithalrao Patil Arts Commerce and Science college Nagaon Tal. And And distt Dhule (M.S)

<sup>2</sup>Madhukar Gangadhar Kasar Smt. N.N.C. Arts Commerce and Science college Kusumba Tal. And distt Dhule (M.S)

<sup>3</sup>Yogita Yadav Government college for Women Pali, Rewari

4-Phenylsulfonyl-2,3,5,6-tetrachloropyridine was synthesized by the reaction of pentachloropyridine with sodium benzenesulfonate under ultrasonic irradiation. This new methodology provides the excellent yield in a very short reaction time at 0 °C. In the presence of ultrasound irradiation, the yield was 90% after 8 min, while was 85% after 10 h by using our previously established method. The substituent effect in *meta* and *para* positions of phenyl ring on intramolecular halogen bond strength was also investigated by theoretical studies. The calculations were performed with Gaussian 09 software at the M05-2X/6-311++G(d,p) level. The results show that one of the oxygen atoms of the SO<sub>2</sub> group is co-planer with the pyridine ring and the other oxygen atom is out of this plane. It was also observed that the electron-withdrawing groups in *meta* and *para* positions reinforce the halogen bond that the oxygen atom of the SO<sub>2</sub> group is co-planer with pyridine ring. An opposite behavior was observed for electron-donating groups.

**Keywords:** Pentachloropyridine, 2,3,5,6-Tetrachloro-4-phenylsulphonylpyridine, Synthesis, Ultrasound irradiation, Halogen bond

## INTRODUCTION

Perchlorinated heteroaromatic compounds have attracted considerable interest in the industry due to their wide range of biological activities such as pesticides and herbicides [1]. Polychloropyridines such as 2,3,5-trichloro-4,6-bis-sulfonylpyridines, tetrachloro-4-sulfonylpyridines, and 3,5-dichloro-2,4,6-tris-sulfonylpyridines have been identified as bactericides [2]; pesticides for controlling bacteria, fungi, crustaceans, insects, nematodes, and weeds [3]. These compounds are also useful in organic syntheses as starting materials for the synthesis of corresponding perfluorinated compounds [4].

During the last two decades, ultrasound is highly regarded in organic syntheses to accelerate a wide number of synthetically useful organic reactions [5]. Recently, we have reported the synthesis of some compounds using ultrasonic irradiation [6]. In the previous paper [7], we have reported the one-pot synthesis of 4-phenylsulfonyl-2,3,5,6-tetrachloropyridine 3 by the reaction of pentachloropyridine

with sodium benzenesulfonate in DMF as a solvent, after stirring at room temperature for 10 h.

Also, many experimental and theoretical studies have been reported on perhalogenated pyridine. Sheu *et al.* studied the structure of 2,3,5,6-tetrafluoropyridine (TFPy) in its ground and excited electronic states using infrared, Raman, and ultraviolet absorption techniques as well as the theoretical calculations. The obtained results showed that the TFPy has a rigid planar structure in its electronic ground state and the structure becomes floppier in the excited state with a small barrier to the planarity of 30 cm<sup>-1</sup> [8]. In 2014, Selvarani *et al.* studied 3-chloro-2,4,5,6-tetrafluoropyridine and 4-bromo-2,3,5,6-tetrafluoropyridine using various theoretical and experimental methodologies, such as thermodynamic and spectral analyses, and density functional theory (DFT)-based analyses using NBO and HOMO-LUMO, and concluded that the theoretical and experimental results are in good agreement with each other [9]. The DFT calculations have been performed on 2-chloro and 3-chloropyridine and 2-bromo- and 3-bromopyridine. The results showed that the N-C bond length in 2-halopyridines is decreased due to the halogen substitution

**Table 1.** Optimization of the Reaction Conditions for the Synthesis of 2,3,5,6-Tetrachloro-4-(phenylsulfonyl)pyridine

Entry	Mole ratio (1:2)	Solvent	Temperature (°C)	Time (min)	Yield (%)
1	1:1	EtOH	r.t.	5	10
2	1:1	CH <sub>3</sub> CN	r.t.	5	40
3	1:1	THF	r.t.	5	20
4	1:1	DMF	r.t.	5	50
5	1:1	EtOH	0	5	Trace
6	1:1	CH <sub>3</sub> CN	0	5	20
7	1:1	THF	0	5	Trace
8	1:1	DMF	0	5	60
9	1:1	DMF	0	8	90
10	1:1	DMF	0	10	90
11	1:2	DMF	0	5	60

on the carbon atom. All of the other ring bond distances for 2-halopyridines and 3-halopyridines were little different from those in pyridine [10].

In this paper, we have synthesized 4-phenylsulfonyl-2,3,5,6-tetrachloropyridine **3** in a very short reaction time with high yield and lower used content of sodium benzenesulfonate using ultrasonic irradiation. Also, the effect of electron-donating (ED) and electron-withdrawing (EW) groups on the strength of intramolecular halogenated bonds in 4-phenylsulfonyl-2,3,5,6-tetrachloropyridine have been studied by theoretical methodologies. We have also investigated the substituent effects on the strength of halogen bond in this molecule using the value of  $\rho$  at halogen bond critical points.

## EXPERIMENTAL

### General Methods

All solvents and starting materials were purchased commercially (Merck). Solvents were dried using the literature procedures and distilled before use. The <sup>1</sup>H NMR spectrum was recorded at 300 MHz. The <sup>13</sup>C NMR spectrum was recorded at 75 MHz. The elemental analyses for C, H and N were performed using Heraeus CHN-O rapid analyzer. TLC analysis was performed on silica gel TLC plates (Merck).

**Synthesis of 2,3,5,6-tetrachloro-4-(phenylsulfonyl)pyridine (3).** Pentachloropyridine **1** (0.251 g, 1 mmol) was added to a solution of sodium benzenesulfonate **2** (0.164 g,

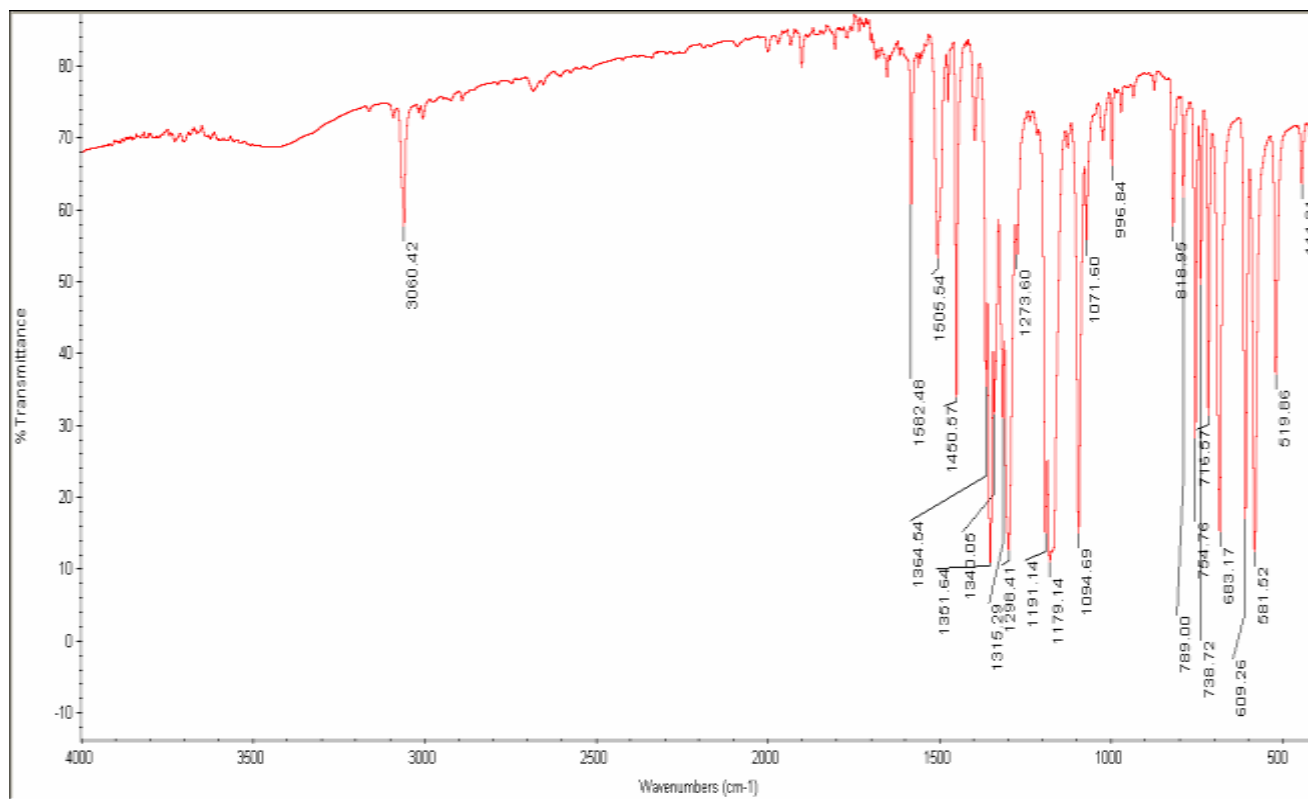


**Fig. 1.** The IR spectrum of 3.

1 mmol) in DMF (5 ml). The reaction mixture was sonicated at 0 °C for 8 min. The precipitate was isolated by filtration. Recrystallization from ethanol gave 2,3,5,6-tetrachloro-4-(phenylsulfonyl)pyridine 3 (0.32 g, 90%) as white crystals; m. p.: 216-219 °C. IR (KBr):  $\nu_{\max}$  1179.1, 1298.4 (SO<sub>2</sub>) cm<sup>-1</sup>. (Found: C, 36.8; H, 1.4; N, 3.7 C<sub>11</sub>H<sub>5</sub>C<sub>14</sub>NO<sub>2</sub>S requires: C, 37.0; H, 1.4; N, 3.9). <sup>1</sup>H NMR (DMSO-d<sub>6</sub>, 300 MHz):  $\delta$  8.06 (d, 2H,  $J$  = 7.36 Hz, Ar-H), 7.86 (t, 1H,  $J$  = 7.56 Hz, Ar-H), 7.72 (t, 2H,  $J$  = 7.48 Hz, Ar-H) ppm. <sup>13</sup>C NMR (DMSO-d<sub>6</sub>, 75 MHz):  $\delta$  149 (Ar-C), 146.8 (Ar-C), 139.3 (Ar-C), 135.8 (Ar-CH), 130.2 (Ar-CH), 129.4 (Ar-C), 128.2 (Ar-CH) ppm.

### Computational Methods

The structures and vibrational frequencies of all complexes were fully optimized by means of M05-2X/6-311++G(d,p) level [11]. All calculations were carried out using the Gaussian 09 [12] suite of programs. The M05-2X method is accurate in the study of individual non-covalent

interactions. The absence of imaginary frequencies shows that the structures are in their ground state.

The topological properties of electron density were obtained using the atoms in molecules (AIM) method [13]. The AIM calculations were performed using the AIM2000 program [14] on the obtained wave functions at M05-2X/6-311++G(d,p) level.

## RESULTS AND DISCUSSION

Initially, we optimized the reaction conditions for the one pot synthesis of 4-phenylsulfonyl-tetrachloropyridine 3 using pentachloropyridine 1 and sodium benzenesulphinate 2 under ultrasonic irradiation (Table 1). For optimization of reaction conditions with respect to the previous method [7], we investigated the effects of solvent, the mole ratio of reactants, reaction time and temperature on the reaction (Table 1). Firstly, the effect of solvent on the yield 3 was evaluated. At room temperature, DMF gave a better result

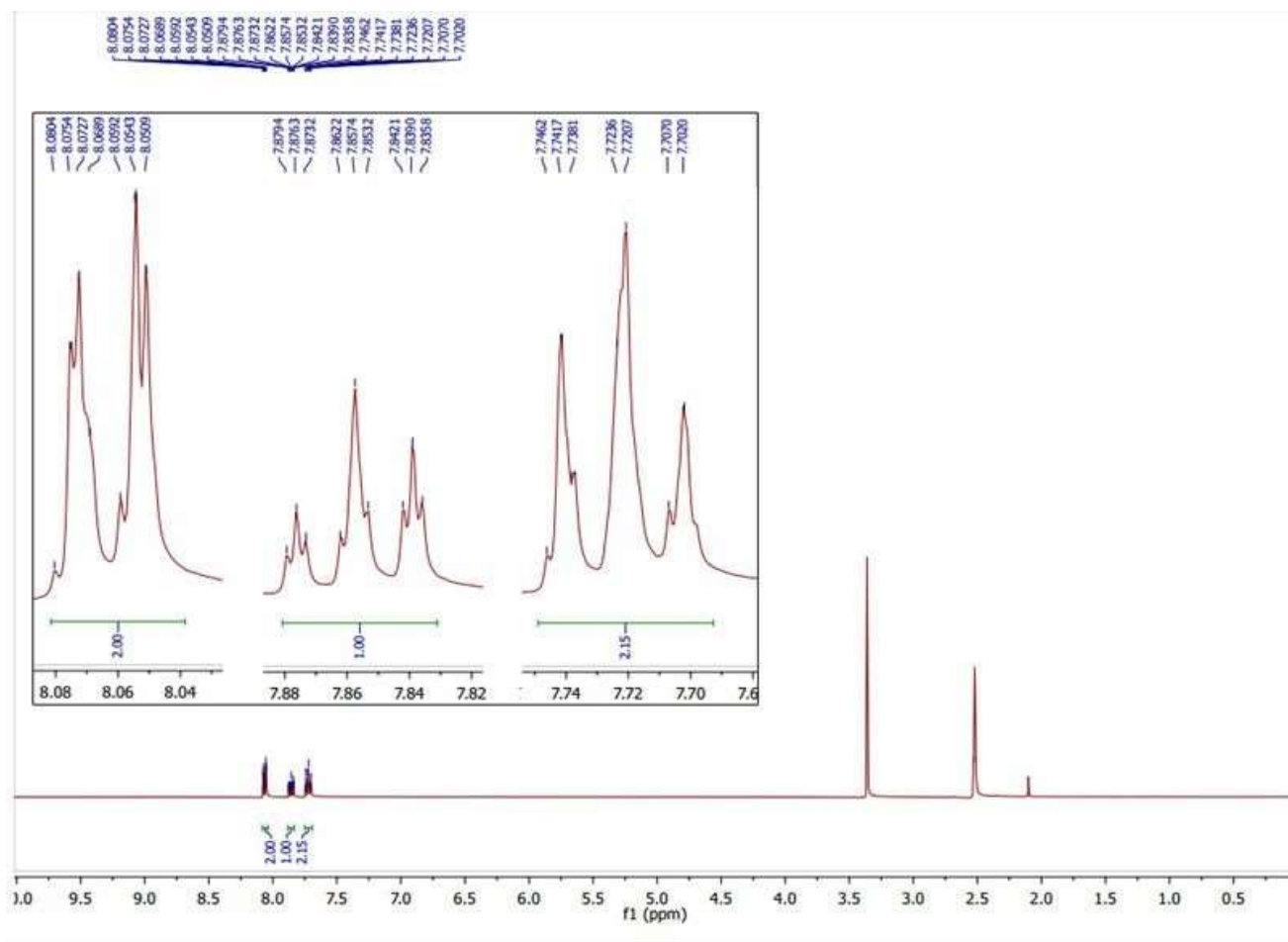


Fig. 2. The  $^1\text{H}$  NMR spectrum of 3.

(Table 1, Entry 4). The highest yield was obtained at  $0^\circ\text{C}$  in DMF (Table 1, Entry 8), and the best yield was obtained at 8 min time reaction (Table 1, Entry 9). Next, we investigated the effect of the mole ratio of reactants that the best yield of 3 was at 1: 1 of the starting materials (Table 1, Entry 9).

The structure of 3 was confirmed with IR, NMR, and elemental analysis. The IR spectrum of 3 showed two absorption bands at  $1179.1$  and  $1298.4\text{ cm}^{-1}$  for  $\text{SO}_2$  stretching (Fig. 1). The  $^1\text{H}$ NMR spectrum of 3 showed a doublet at  $8.06\text{ ppm}$  and two triplets at  $7.86$  and  $7.72\text{ ppm}$  for aromatic H (Fig. 2). In the  $^{13}\text{C}$  NMR spectrum, aromatic carbons were located at  $149$ ,  $146.8$ ,  $139.3$ ,  $135.8$ ,  $130.2$ ,  $129.4$  and  $128.2\text{ ppm}$  (Fig. 3). The phenylsulfonyl group is a strong electron withdrawing group that helps maintain the reactivity of pyridine ring toward further nucleophilic

substitution processes. This allows annelation and further functionalization to proceed.

### Theoretical Calculations

**Geometrical parameters.** In order to compare the effect of electron-donating (ED) and electron-withdrawing (EW) groups on the strength of intramolecular halogenated bonds in 4-phenylsulfonyl-2,3,5,6-tetrachloropyridine 3, the binding energy of atoms in 4-phenylsulfonyl-tetrachloropyridine 3 with the different substituents on the phenyl ring was obtained using the following formula:

$$BE = \frac{([aE_C + bE_N + cE_F + dE_H + eE_O + fE_{Cl} + gE_S + hE_{Br}] - E_{Complex})}{(a + b + c + d + e + f + g + h)}$$

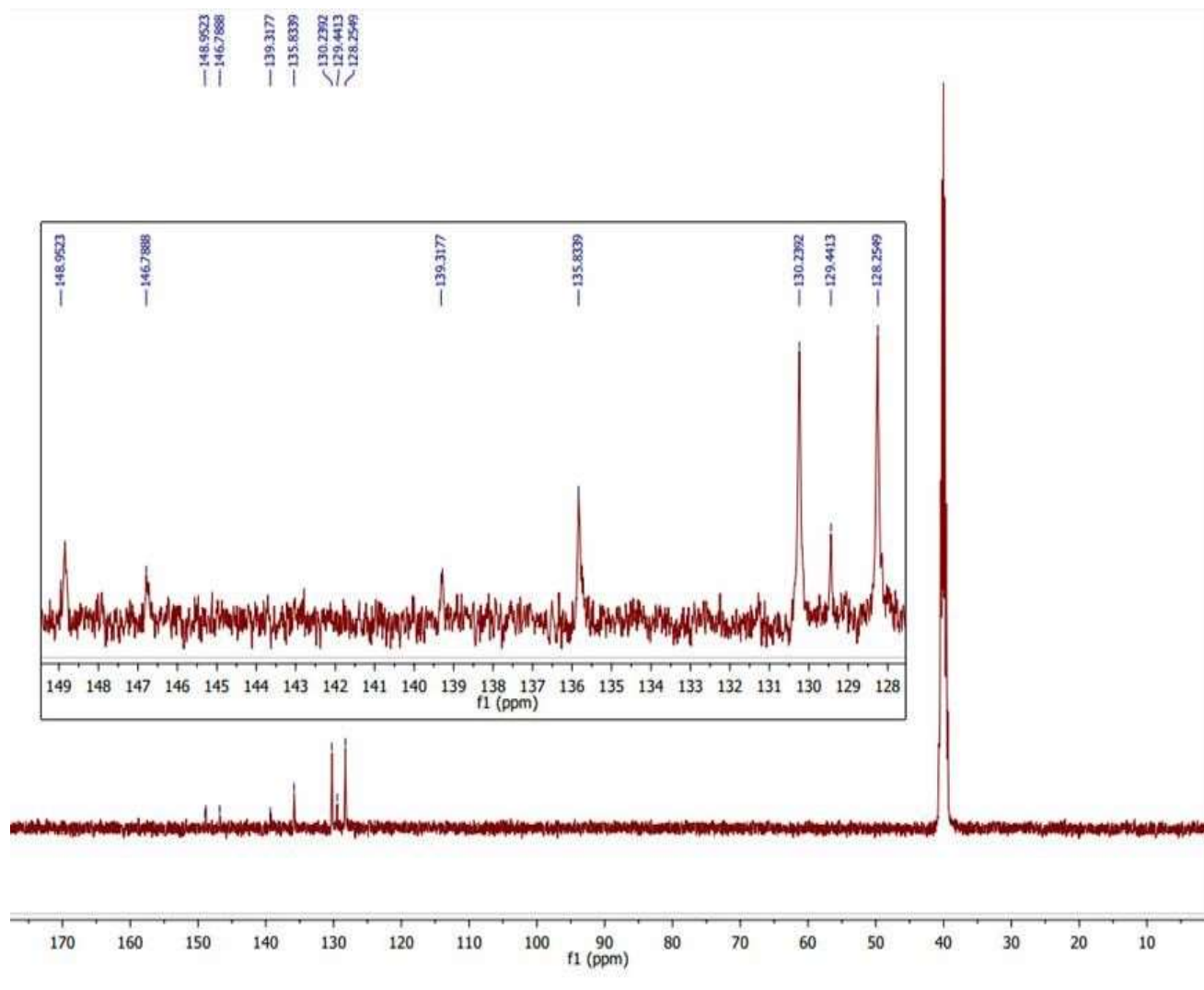


**Fig. 3.** The  $^{13}\text{C}$  NMR of 3.

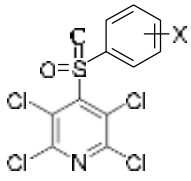
where BE is binding energy,  $E_{\text{C}}$ ,  $E_{\text{N}}$ ,  $E_{\text{F}}$ ,  $E_{\text{H}}$ ,  $E_{\text{O}}$ ,  $E_{\text{Cl}}$ ,  $E_{\text{S}}$ ,  $E_{\text{Br}}$  are the energy of atoms C, N, F, H, O, Cl, S, Br and  $E_{\text{Complex}}$  is energy of the studied complex, respectively, at the M05-2X/6-311++G(d,p) level of theory. Coefficients a, b, c, d, e, f, g and h represent the number of atoms in the corresponding complex. The binding energy values in both *meta* and *para* positions are gathered in Table 2.

The order of binding energy in both *meta* and *para* positions are as follows:



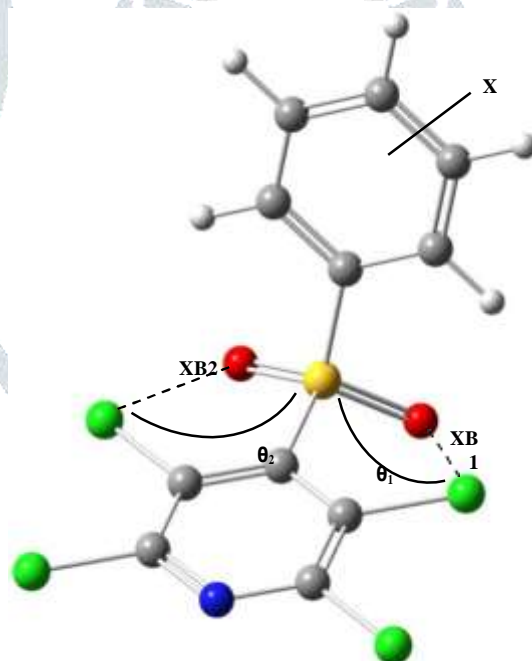
As can be seen, the complexes containing EW groups are more stable than those of ED groups. The calculations showed that one of the oxygen atoms of the  $\text{SO}_2$  group is co-planer with the pyridine ring and the other oxygen atom is out of this plane. As shown in Scheme 1, they are marked by XB1 and XB2, respectively. The important structural parameters required for the description of the halogen bond in both positions are given in Table 2. These parameters include halogen bond lengths and halogen bond angles.

The XB1 bond length in *meta* position lies in the range of 2.788–2.918 Å, which the shortest and highest bonds

**Table 2.** The Values of BE (kJ mol<sup>-1</sup>), Halogen Bond Distances (Å) and Bond Angles (°) in the studied complexes<sup>a</sup>


X	BE	XB1	XB2	$\theta_1$	$\theta_2$
CF <sub>3</sub>	107.827, <b><i>107.828</i></b>	2.793, <b><i>2.787</i></b>	2.917, <b><i>3.018</i></b>	100.491, <b><i>101.164</i></b>	89.417, <b><i>84.199</i></b>
CH <sub>3</sub>	106.466, <b><i>106.480</i></b>	2.794, <b><i>2.794</i></b>	2.915, <b><i>2.907</i></b>	100.679, <b><i>100.498</i></b>	89.679, <b><i>90.272</i></b>
CN	110.818, <b><i>110.825</i></b>	2.788, <b><i>2.787</i></b>	2.966, <b><i>2.969</i></b>	101.100, <b><i>101.165</i></b>	86.538, <b><i>86.377</i></b>
N(CH <sub>3</sub> ) <sub>2</sub>	103.924, <b><i>103.992</i></b>	2.801, <b><i>2.798</i></b>	2.884, <b><i>2.881</i></b>	99.818, <b><i>99.916</i></b>	91.992, <b><i>92.188</i></b>
NO <sub>2</sub>	108.747, <b><i>108.742</i></b>	2.791, <b><i>2.790</i></b>	2.988, <b><i>2.986</i></b>	101.030, <b><i>101.068</i></b>	85.355, <b><i>85.511</i></b>
OCH <sub>3</sub>	105.826, <b><i>105.891</i></b>	2.918, <b><i>2.792</i></b>	2.792, <b><i>2.905</i></b>	89.481, <b><i>100.597</i></b>	100.688, <b><i>90.385</i></b>
H	107.450	2.916	2.792	89.563	100.694

<sup>a</sup>The bold and italic data is corresponding to *para* position.



*Scheme 1.* The investigated complexes in the present work  
 X = H, CN, CF<sub>3</sub>, NO<sub>2</sub>, CH<sub>3</sub>, N(CH<sub>3</sub>)<sub>2</sub>, OCH<sub>3</sub>

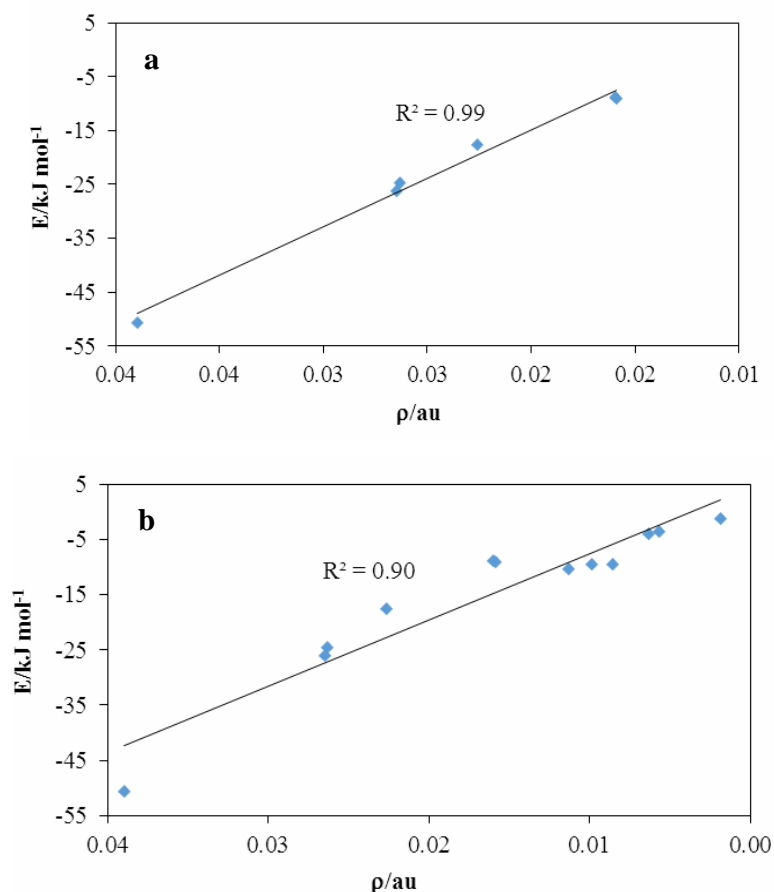


**Fig. 4.** The linear correlation between  $\Delta E$  values and  $\rho$ : a)  $H_2Y \cdots H-X$ ; b)  $H_2Y \cdots H-X$  and  $H_2Y \cdots X-H$  ( $X = F, Cl, Br, Y = S, O$ ) complexes.

related to  $CN$  and  $OCH_3$ , respectively. Moreover, the data presented in Table 2 showed that the EW and ED groups cause to shorten and lengthen the halogen bond, respectively. Consequently, the XB2 halogen bond in this position is in the range of 2.792–2.988 Å that are the least and most values related to  $OCH_3$  and  $NO_2$  substituents, respectively. According to Table 2, the halogen bond length decreases or increases by the EW and ED groups. As a result, the behavior of EDGs and EWGs is reversed on XB1 and XB2 bonds.

According to Table 2, the EDGs and EWGs strengthen and weaken the XB1 bond length in the *para* position. The opposite behavior is observed for XB2.

AIM calculations were done on the structure of the mentioned complexes at the M05-2X/6-311++G(d,p). In

order to investigate the strength of hydrogen bonds, empirical Espinosa-Molins-Lecomte formula (EML) [15] is used. This equation is based on the electron density distribution in the critical point of hydrogen bonding:

$$E_{EML,HB} = 0.5 \times V(r)$$

To estimate the strength of individual halogen bond in the studied complexes, the six complexes of  $H_2Y \cdots H-X$  ( $X = F, Cl, Br, Y = S, O$ ) were selected. Optimization of structures was performed at M05-2X/6-311++G(d,p). The AIM calculations were performed on six complexes and  $\rho$  values were extracted. Hydrogen bonding energy was calculated using the EML formula. The plot of  $E$  versus  $\rho$  was drawn for these complexes and the amount of correlation

**Table 3.** Topological Properties of Electron Density (in a.u.) at the Bond Critical Point of X-bonds and Values of H-bond Energy ( $\text{kJ mol}^{-1}$ ) Estimated by EML Formula<sup>a</sup>

X	XB1				XB2			
	$\rho \times 10^2$	$\nabla^2\rho \times 10^2$	$H \times 10^2$	$E_{\text{EML}}$	$\rho \times 10^2$	$\nabla^2\rho \times 10^2$	$H \times 10^2$	$E_{\text{EML}}$
CF <sub>3</sub>	1.967	7.650	0.178	-0.778	1.634	5.930	0.133	-0.609
	(1.987)	(7.738)	(0.180)	(-0.788)	(1.418)	(4.952)	(0.114)	(-0.505)
CH <sub>3</sub>	1.962	7.634	0.178	-0.776	1.635	5.964	0.136	-0.610
	(1.966)	(7.639)	(0.176)	(-0.778)	(1.655)	(6.059)	(0.137)	(-0.620)
CN	1.980	7.723	0.181	-0.784	1.525	5.407	0.121	-0.555
	(1.986)	(7.743)	(0.181)	(-0.787)	(1.519)	(5.390)	(0.122)	(-0.552)
N(CH <sub>3</sub> ) <sub>2</sub>	1.949	7.514	0.170	-0.769	1.706	6.328	0.145	-0.646
	(1.958)	(7.573)	(0.173)	(-0.774)	(1.720)	(6.372)	(0.143)	(-0.653)
NO <sub>2</sub>	1.970	7.683	0.182	-0.779	1.483	5.210	0.117	-0.535
	(1.976)	(7.694)	(0.180)	(-0.783)	(1.484)	(5.224)	(0.118)	(-0.535)
OCH <sub>3</sub>	1.627	5.921	0.134	-0.606	1.975	7.659	0.176	-0.782
	(1.973)	(7.672)	(0.177)	(-0.782)	(1.659)	(6.072)	(0.137)	(-0.622)
H	1.633	5.940	0.134	-0.609	1.973	7.657	0.176	-0.781

<sup>a</sup>The data in parentheses is corresponding to *para* position.

coefficient was obtained equal to 0.99. In the following, the complexes  $\text{H}_2\text{Y}\cdots\text{X-H}$  ( $\text{X} = \text{F}, \text{Cl}, \text{Br}, \text{Y} = \text{S}, \text{O}$ ) was optimized at the M05-2X/6-311++G(d,p) level. Then, the AIM calculations were performed on these complexes in order to extract the  $\rho$  values. Similar to hydrogen bonds, the EML formula was used to estimate the separate halogen bond. The chart of  $E$  versus  $\rho$  for halogen ( $\text{H}_2\text{Y}\cdots\text{X-H}$ ) and hydrogen ( $\text{H}_2\text{Y}\cdots\text{H-X}$ ) bonds was drawn in one graph. The correlation coefficient is equal to 0.90. These results indicate that EML formula can be used to estimate the halogen bond energy.

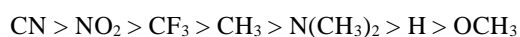
The values of  $\rho$ ,  $\nabla^2\rho$ ,  $H(r)$ ,  $V(r)$  and  $E_{\text{EML}}$  for XB1 and XB2 bonds, derived from AIM calculations for *meta* and *para* positions, are represented in Table 3. Nakanishi *et al.* recently used the method of analysing the behavior of local electron density ( $H$ ) in terms of the Laplacian of the electron density ( $\nabla^2\rho$ ) at the bond critical point to classify

the strength of the Non-covalent bonds [16]. Laplacian sign of the electron density ( $\nabla^2\rho$ ) which is the second derivative of the electron density at the bond critical points represents localization or delocalization of electron density between the nuclei of two atoms involved in the reaction. However, total electron density ( $H$ ) reflects the stability or instability of the local distribution of the electrons at the bond critical points. Accordingly, if  $\nabla^2\rho$  smaller than zero, the electron density at the bond critical point is higher than that in the other bond critical points, which is said the bond has the shared-shell property. In the case that  $\nabla^2\rho$  is greater than zero, in addition to revealing the nature of the closed-shell bond, indicates the fact that the local bond critical point is the region with low localization of electron density.

The role of the local distribution of electron density ( $H$ ) is remarkable in the determination of bond nature. It is said that the bond has pure closed-shell property, if the local

distribution of the electron density is positive at the bond critical point. On the other hand, if the value of local electron density at the bond critical point is negative,  $H < 0$ , it can be said that it has regular closed-shell property. This feature of bonds lies in the area between closed-shell and pure closed-shell and is distinguished from the other area with the stable distribution of electron. As can be seen,  $\nabla^2\rho$  and  $H$  are positive in both the XB1 and XB2 bond at the *meta* and *para* positions, and thus they are located in the region of pure closed-shell. In the other words, it can be concluded that the electron density at the bond critical point is unstable ( $H > 0$ ) and is not localized at this critical point ( $\nabla^2\rho > 0$ ).

The trend of  $\rho$  values for XB1 in *meta* position as follows:



In fact, the amount of electron density increases by increasing the EW strength of substituents. This order indicates that the halogen bond is strengthening by EW substituents.

As indicated in Table 3, the ED and EW groups increase and decrease the amount of  $\rho$  at XB2, respectively, in this position. These results are in agreement with the structural parameters.

Also, the value of  $\rho$  at XB1 increases with increasing EW strength of substituents in the *para* position. This behavior is reversed for XB2 in this position. Thus, the halogen bond strength increases and decreases with increasing ED groups for XB1 and XB2, respectively.

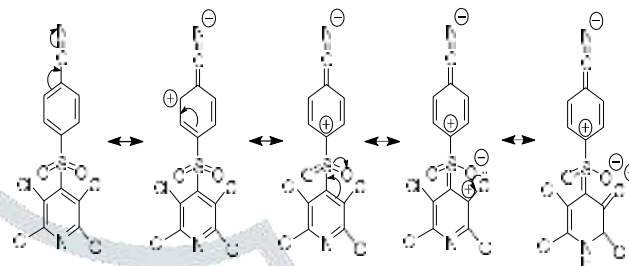
As shown in Table 3, the trend in  $|E_{\text{EML}}|$  is similar to that for  $\rho$  at XB1 and XB2 bonds in *meta* and *para* positions. Therefore, XB1/XB2 halogen bond strength increases by EW/ED strength in both positions. A meaningful relationship can be found between  $E_{\text{EML}}$  and  $\rho$  in *para* and *meta* position.

According to the AIM results and structural data, these changes in *para* and *meta* positions can be explained as follows:

Electron-withdrawing groups with  $\pi$  bonds to electronegative atoms (*e.g.*  $-\text{C}\equiv\text{N}$ ) adjacent to the  $\pi$  system deactivate the aromatic ring by decreasing the electron density on the ring through a resonance withdrawing effect. The resonance decreases the electron density at *ortho* and

*para* positions. Substituents with several bonds to electronegative atoms (*e.g.*  $-\text{CF}_3$ ) adjacent to the  $\pi$  system deactivate the aromatic ring by decreasing the electron density on the ring through an inductive withdrawing effect. The net overall effect is similar to that described above for other electron withdrawing groups.

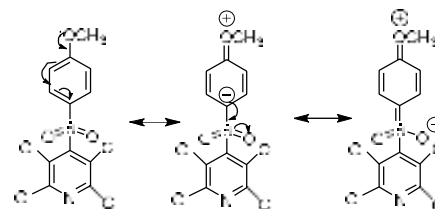
The electron-withdrawing groups, for example  $-\text{CN}$ , resonate in the *para* position with the oxygen atom that is co-planer with pyridine ring as follows:



Consequently, Cl and O atoms have positive and negative charges, respectively, and the halogen bond, formed with the oxygen atom that is co-planer with pyridine ring, is stronger than the other halogen bond.

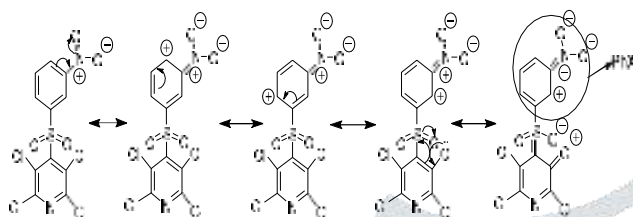
Electron-donating groups with lone pairs (*e.g.*  $-\text{OCH}_3$ ) on the atoms adjacent to the  $\pi$  system activate the aromatic ring by increasing the electron density on the ring through a resonance donating effect. The resonance allows electron density to be positioned at the *ortho* and *para* positions. Hence, these sites are more nucleophilic, and the system tends to react with electrophiles at these sites. Alkyl substituents (*e.g.*  $-\text{CH}_3$ ,  $-\text{CH}_2\text{CH}_3$ ) are also electron donating groups. They activate the aromatic ring by increasing the electron density on the ring through an inductive donating effect.

The electron-donating groups, for example  $\text{OCH}_3$ , resonate in the *para* position with the oxygen atom that is co-planer with pyridine ring as follows:

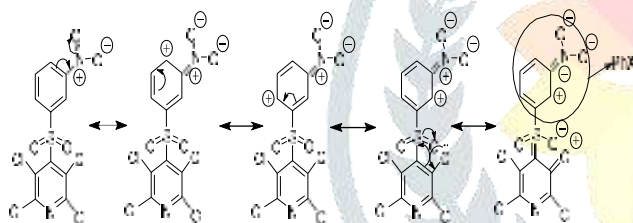


As a result, the negative charge density increases on the oxygen atom. Also, in C–Cl bond, Cl atom is more electronegative than C atom, and it creates a partial negative charge on Cl atom. Thereby, created repulsion between the adjacent negative charges causes the formed halogen bond to become weak.

The resonance forms of electron-withdrawing groups for example NO<sub>2</sub> in *meta* position with the oxygen located in the same plane of pyridine ring is as follows:



PhX group plays an inductive role and thus increases the contribution of halogen to the resonance and formation of the final resonance form. In this form, Cl atom finds positive charge and formed halogen bond becomes stronger than other halogen bonds. The resonance of electron-donating groups such as OCH<sub>3</sub> with the oxygen atom in the *meta* position is as follows:



Here, PhX has a donating role and thus gives electrons to the SO<sub>2</sub> group by induction. Thus, negative carbon orbitals overlap with the positive empty orbitals of sulfur. Thereby, it reinforces the halogen bond which its oxygen atom is placed out of the pyridine ring plane.

## CONCLUSIONS

We have synthesized 4-phenylsulfonyl-2,3,5,6-tetrachloropyridine in a very short reaction time with high yield

and lower used content of sodium benzenesulfonate using ultrasonic irradiation. The quantum chemical calculations were performed on 4-phenylsulfonyl-2,3,5,6-tetrachloropyridine, in which substituents were placed at *meta* and *para* positions of the phenyl ring. On the basis of the results, one of the oxygen atoms of the SO<sub>2</sub> group is co-planer with pyridine ring (XB1), while another oxygen atom is located out of this plane (XB2). According to the structural data, the energy of the halogen bond, and AIM results, the EW and ED groups in both positions respectively weaken and strengthen the XB1 halogen bond in both positions. The opposite behavior was observed for XB2. The excellent correlations were found between the energy data, structural parameters and the results of AIM analysis.

## ACKNOWLEDGMENTS

We gratefully acknowledge, the Vail-e-Asr University of Rafsanjan Faculty Research Grant for financial support.

## REFERENCES

- [1] H. Suschitzky, Polychloroaromatic Compounds, Plenum Press London, New York, 1974.
- [2] D. Kyriacou, Chem. Abstr. 82, 1975, 43181; Dow Chemical Co. US 3,829,430.
- [3] C.J. Gilmore, D.D. MacNicol, A. Murphy, M.A. Russell, Tetrahedron Lett. 25 (1984) 4303.
- [4] R.D. Chambers, J. Hutchinson, W.K.R. Musgrave, J. Chem. Soc. (1964) 3573.
- [5] a) S.J. Doktycz, K.S. Suslick, Science 247 (1990) 1067; b) T. Mason, J. Chem. Soc. Rev. 26 (1997) 443; c) G. Cravotto, P. Cintas, Chem. Soc. Rev. 35 (2006) 180; d) H. Fillion, J. L. Luche, In Synthetic Organic Sonochemistry; Ed.; Plenum: New York, NY, 1998; e) R. Cella, H.H. Stefani, Tetrahedron 65 (2009) 2619.
- [6] a) R. Ranjbar-Karimi, M. Mashak-Shoshtari, A. Darehkordi, Ultrason. Sonochem. 18 (2011) 18 258; b) R. Ranjbar-Karimi, Ultrason.Sonochem. 17 (2010) 768; c) A. Poorfreidoni, R. Ranjbar-Karimi, R. Kia, New J. Chem. 39 (2015) 4398.
- [7] R. Ranjbar-Karimi, A. Poorfreidoni, J. Iran. Chem. Soc. 14 (2017) 933.

- [8] H.L. Sheu, P. Boopalachandran, S. Kim, J. Laane, Chem. Phys. 456 (2015) 28.
- [9] C. Selvarani, V. Balachandran, K. Vishwanathan, Spectrochim. Acta Mol. Biomol. Spectrosc. 132 (2014) 110.
- [10] P. Boopalachandran, H.L. Sheu, J. Laane, J. Mol. Struct. 1023 (2012) 61.
- [11] E.G. Hohenstein, S.T. Chill, C.D. Sherrill, J. Chem. Theory Comput. 4 (2008) 1996.
- [12] M.J. Frisch, G.W. Trucks, H.B. Schlegel, G.E. Scuseria, M.A. Robb, J.R. Cheeseman, D.J. Fox, Gaussian 09 (Revision A.02), Gaussian, Wallingford, CT, 2009.
- [13] R.F.W. Bader, A Suite of Programs for the Theory of Atoms in Molecules, Hamilton, Canada, in: Atoms in Molecules: A. Quantum Theory, vol. 75, Oxford University Press, Oxford, 1990, pp. 1-49.
- [14] F. BieglerKönig, J. Schönbohm, J. Comput. Chem. 23 (2002) 1489.
- [15] E. Espinosa, E. Molins, C. Lecomte, Chem. Phys. Lett. 285 (1998) 170.
- [16] W. Nakanishi, S. Hayashi, Curr. Org. Chem. 14 (2010) 181.

